Geological Society of America
Special Paper 369
2003

Paleoproductivity of the northwestern Tethyan margin (Anthering Section, Austria) across the Paleocene-Eocene transition

Hans Egger
Geologische Bundesanstalt, Rasumofskygasse 23, Austria, 1031 Wien
Juliane Fenner
Bundesanstalt für Geowissenschaften und Rohstoffe, Postfach 510153, Germany, 30631 Hannover
Claus Heilmann-Clausen
Geologisk Institut, Aarhus Universitet, Denmark, 8000 Aarhus C
Fred Rögl
Naturhistorisches Museum, Burgring 7, Austria, 1010 Wien
Reinhard F. Sachsenhofer
Universität Leoben, Institut für Geowissenschaften, Franz-Josef-Strasse 18, Austria, 8700 Leoben
Birger Schmitz
Department of Earth Sciences, Marine Geology, Göteborg University, SE 405 30 Göteborg, Sweden

ABSTRACT

Sediments in the expanded Anthering Section at the northwestern Tethyan margin were deposited in an abyssal environment, at the continental rise to the south of the European plate. The section contains deposits from calcareous nannoplankton Zones NP9 and NP10 and displays the global negative carbon isotope excursion (CIE) in the upper part of Zone NP9. Associated with the CIE is a strong three-fold increase in the rate of hemipelagic sedimentation. This suggests an increased input of siliciclastic suspended material into the basin, which is indicative of enhanced continental runoff at that stratigraphic level. Concurrent acmes of siliceous plankton and dinoflagellate cysts indicate that a high input of dissolved nutrients affected even open marine settings and caused eutrophication of surface waters. The associated high flux of organic carbon to the seafloor resulted in oxygen-depleted conditions and caused the total extincton of benthic faunas. However, impoverished foraminifera faunas indicate that a change of ecological conditions started shortly before the CIE.

INTRODUCTION

A prominent decrease in the $^{13}C/^{12}C$ ratio of global carbon reservoirs (negative carbon isotope excursion—CIE) took place ca. 55 Ma ago, and is explained as the result of massive methane release due to the dissociation of gas hydrates (see Katz et al., 1999, for a review). This process may have been triggered by a rise in ocean bottom water temperature of between 4 and 8 °C which can be inferred from oxygen isotope values of foraminifera (e.g., Kennett and Stott, 1991). Coeval intense deep-sea carbonate dissolution indicates a shoaling of the calcite compensation depth as a result of the oxidation of methane to carbon dioxide (Dickens et al., 1995). The CIE is associated with a global extinction event of deep-sea benthic foraminifera (see

---

*E-mails: Egger—eggjoh@cc.geolba.ac.at; Fenner—J.Fenner@bgr.de; Heilmann-Clausen—claus.heilmann@geo.au.dk; Rögl—fred.roegl@nhm-wien.ac.at; Sachsenhofer—sachsenh@unileoben.ac.at; Schmitz—birger@gvc.gu.se.

Egger, H., Fenner, J., Heilmann-Clausen, C, Rögl, F., Sachsenhofer, R.F., Schmitz. B., 2003, Paleoproductivity of the northwestern Tethyan margin (Anthering Section, Austria) across the Paleocene-Eocene transition, *in* Wing, S.L., Gingerich, P.D., Schmitz, B., and Thomas, E., eds., Causes and Consequences of Globally Warm Climates in the Early Paleogene: Boulder, Colorado, Geological Society of America Special Paper 369, p. 133–146.

Thomas, 1998, for a review), a rapid diversification of planktonic foraminifera (Lu and Keller, 1993), a global bloom of the dinoflagellate genus *Apectodinium* (Crouch et al., 2001), a turnover in calcareous nannoplankton (Bybell and Self-Trail, 1994), and a major turnover in land mammals (Wing et al., 1991). In the South Atlantic and Antarctica and in some Tethyan sections a high influx of kaolinite has been interpreted as an indicator for a change to more humid climatic conditions or, alternatively, as an effect of enhanced erosion under more arid conditions (see Thiry, 2000, for a review).

Over extensive areas in the southern and northern Tethys and Peri-Tethys, the CIE is coeval with sapropelic sedimentation (Speijer et al., 1997; Gavrilov et al., 2000; Schmitz et al., 1997a). Biogenic barium, which can be used as a proxy for paleoproductivity, indicates a dramatic increase in surface water fertility in the Eastern Tethys (Schmitz et al., 1997b) and in the North and South Atlantic (Bains et al., 2000). However, studies of microfossil assemblages, including these at sites where elevated barite accumulation has been documented, suggest that surface productivity actually decreased during the $\delta^{13}C$ excursion (Dickens et al., 2001). From the expanded and continuous sedimentary record of the Anthering Section (Fig. 1) an acme of siliceous plankton (Egger et al., 2000b) can be interpreted either as an indicator of high surface-water productivity or as a result of better preservation conditions for siliceous plankton.

The main objective of this paper is to explore the significance of the faunal and floral changes at the level of the CIE at Anthering. Since the influx of suspended terrestrial material into the basin is essential for the preservation of organic matter as well as for the level of dissolved nutrients in the surface water, we calculated hemipelagic sedimentation rates that can be used as a proxy for the amount of fluvial discharge. We studied temporal relationships between high sedimentation rates, acmes of planktic assemblages and the benthic foraminifera extinction event (BFEE). In order to discriminate between effects of preservation and signals of changed primary productivity, we focus on the ecological significance of *Apectodinium* and large diatom species (*Trinacria* spp. and *Craspedodiscus* spp.).

ENVIRONMENTAL SETTING

The 250 m thick upper Paleocene to lower Eocene deposits of the Austrian Anthering Section, spanning calcareous nannoplankton Zones NP9 and NP10, represent the most expanded marine sedimentary record of this interval known to date. These sediments comprise the youngest part of the Rhenodanubian Flysch that was deposited on the continental rise to the south of the European plate (Fig. 2), which was the main source for the siliciclastic detritus entering the basin. The section is composed of carbonaceous mud-turbidites with intervening hemipelagic shales, which indicate deposition below the calcite compensation depth. Paleo-water depth estimations by Butt (1981), using foraminifera assemblages, range between 3000 and 5000 m.

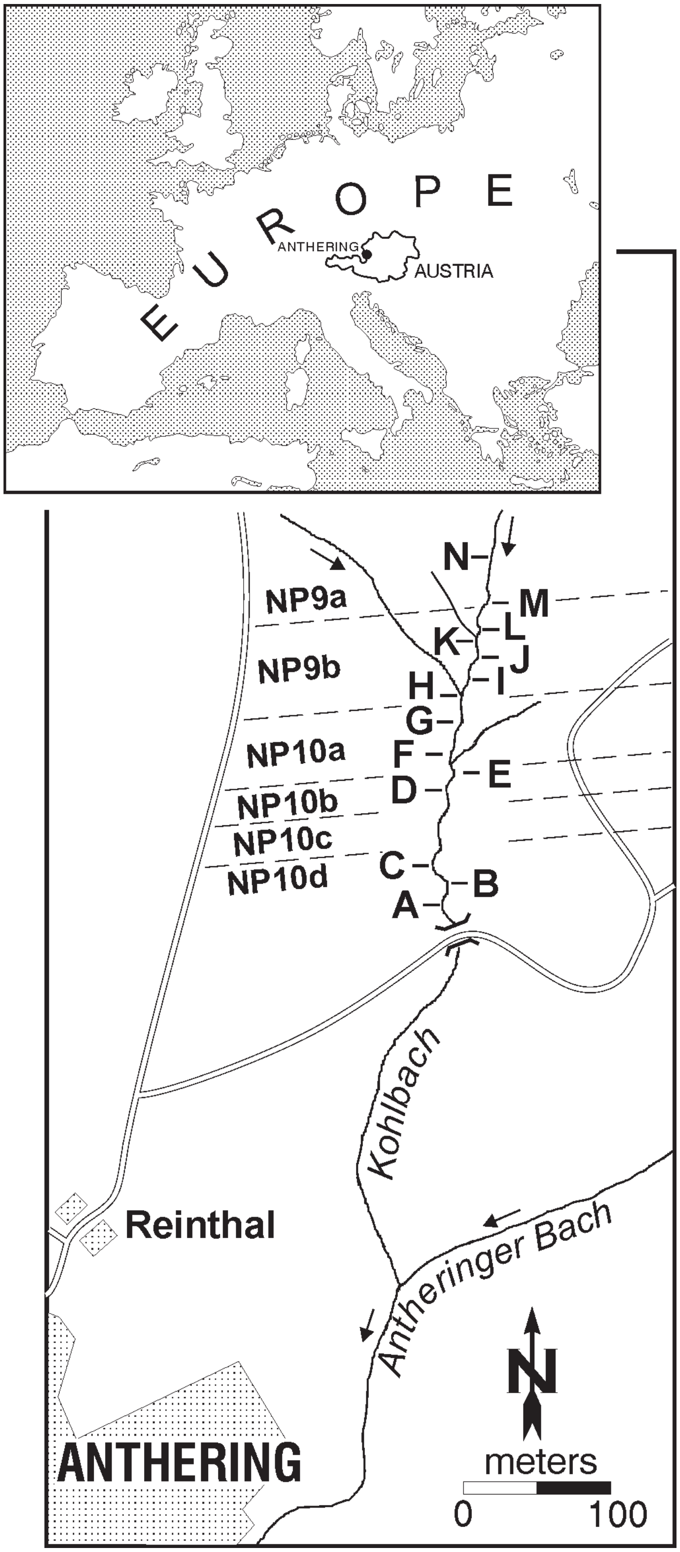

Figure 1. Position of the Anthering section, location of outcrops (A–N) and biostratigraphy of outcrops in terms of the calcareous nannoplankton standard zonation (NP Zones) of Martini (1971) and their further subdivision by Aubry (1996).

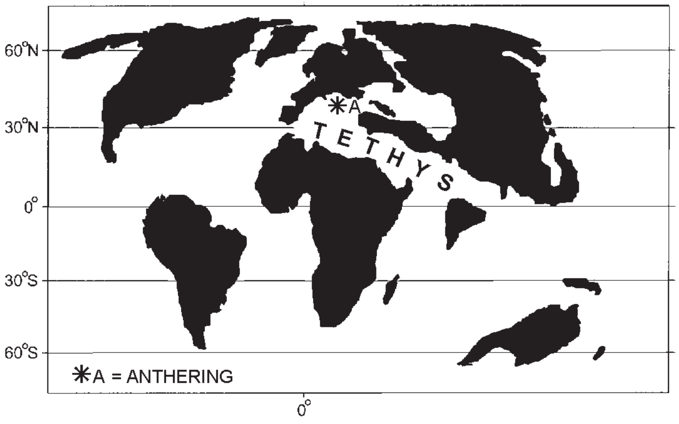

Figure 2. Paleogeographic reconstruction for the late Paleocene (modified from Scotese and Golanka, 1992) showing the location of Anthering.

For the Paleogene, a warm seasonal climate with alternating wet and dry conditions is indicated by the strong dominance of smectite in the clay mineral assemblages of hemipelagic shale. Close to the CIE, slightly increased percentages of kaolinite suggest a change to a more humid climate with high precipitation rates and associated enhanced continental runoff (Egger et al., 2002). This interpretation is consistent with terrestrial palynomorph assemblages in samples taken immediately above the onset of the CIE. These contain elements of the subtropical/tropical vegetation similar to the recent flora of Southeast Asia and southeast North America (Draxler, 2000).

SAMPLES AND METHODS

The stratigraphical framework of our study is based on the standard nannofossil zonation of Martini (1971), the subdivision of Zone NP10 by Aubry (1996) and the position of the CIE in the upper part of zone NP9 (Egger et al., 2000a). To show the temporal variations in turbidity current frequency, we counted the number of turbidite beds per meter of hemipelagic interturbidite sediment (Gawenda et al., 1999). These sediments are devoid of carbonate and, therefore, can be easily distinguished from carbonate-bearing turbidites (see Hesse, 1975, for a review). Additionally, we measured logs at a the scale of 1:10 to assess the number of turbidites and the percentages of hemipelagic shale. Since only ~40% of the entire Anthering Section is exposed, we extrapolated these results to the complete thicknesses of the nannoplankton subzones to calculate the compacted hemipelagic and turbiditic sedimentation rates.

For micropaleontological, clay mineralogical and organic geochemical studies we made splits of the same 33 hemipelagic samples, these were taken at least 10 cm below the outcrop surface. Total organic carbon (TOC) contents were determined on decarbonated samples using a LECO 300 CS^{TM} analyzer. Additionally, Rock Eval analyses (Espitalié et al., 1977) of 10 whole rock samples with increased percentages of organic matter were performed in duplicate using a Rock-Eval II+ instrument. Standard notations are used: S1 and S2 in milligrams of hydrocarbons (HC) per gram of rock; Tmax expressed in °C and the total organic carbon in wt%. The hydrogen index (HI = 100*S2/TOC) and oxygen index (OI = 100*S3/TOC) are expressed in mgHC/gTOC and mgCO$_2$/gTOC. Semiquantitative maceral evaluation of samples with a TOC content of >1% was performed using whole rock samples orientated perpendicular to bedding and a point counter. Between 500 and 1000 points per polished block were analysed using reflected white light and blue light excitation. Vitrinite reflectance was determined following established procedures and using a Leitz MPV-SP microscope.

Absolute dinoflagellate cyst abundances (cysts per gram sediment) were calculated following the method of Stockmarr (1971) which involves the addition of tablets with a known number of Lycopodium spores to the sediment samples during palynological processing. Semiquantitative abundances of agglutinating foraminifera and siliceous plankton from sieving residues (>125 µm) were determined from 32 shale samples. 200 g of each sample were processed for these analyses. In addition, the smaller size fractions were checked for remains of diatoms by treating the bulk sediment sample with 10% flouric acid and by further concentration using heavy liquid separation. Beside the taxonomic determination of the diatom valves, the relative abundance of the remains of the different siliceous microfossil groups and their preservation were examined. The samples were analysed with a lightmicroscope at a magnification of 1000x and with a scanning electron microscope.

For the palecological interpretation the deep water agglutinating foraminfera (DWAF) were grouped into assemblages (“morphogroups”) according to modern analogues of life habitats and feeding strategies (e.g., Jones and Charnock, 1985; Kaminski et al., 1989; Kaminski et al., 1999). The diversity of DWAF has been calculated by using the Shannon-Wiener index (Lipps et al., 1979).

RESULTS

Sedimentation rates

The onset of the CIE is characterized by the presence of the thickest hemipelagic layers of the entire Anthering Section. About 45% of the rocks in the upper part of NP9 are shales, whereas the average percentage of shales in the overlying NP10 is only 14%, and even less in the lower part of NP9. The threefold increase in shale thickness can be explained either as a result of a decrease in the frequency of turbidity currents entering the basin or as a result of enhanced hemipelagic sedimentation. Sedimentation rates for the entire Anthering Section, incorporating both the turbidites and the hemipelagites, have been estimated as 9.1 cmky^{-1} (Egger et al., 2000a). The sedimentation rate for the hemipelagic shale has been estimated as 1.8 cmky^{-1}.

As this rate can be used as a proxy for the amount of fluvial discharge, we tried to get a better resolution by assessing this rate for the individual nannoplankton subzones of the section.

A fourfold subdivision of calcareous nannoplankton zone NP10 has been proposed by Aubry (1996) who estimated the duration of the subzones 10a, 10b 10c and 10d as 630 k.y., 200 k.y., 240 k.y., and 320 k.y. For zone NP9 we used estimations by Aubry et al. (1996) who calculated the duration of this zone as 1 Ma and the position of the CIE as 530 k.y. above the base of NP9.

Using these estimations we have calculated the rate of hemipelagic sedimentation (Fig. 3) as 1.3 cm/k.y. for the lower part of zone NP9 (120 m thick below the CIE), as 4.3 cm/k.y. for the upper part of NP9 (45 m thick), as 1.3 cm/k.y. for NP10a (50 m thick), as 0.9 cm/k.y. for NP10b (12 m thick) and as 0.7 cm/k.y. for NP10c (16 m thick). The sediments of subzone NP10d attain a thickness of 25 m, however, in contrast to previously published results (Egger et al., 2000a), we found *Tribrachiatus contortus* in our new samples from the very top of the section, suggesting

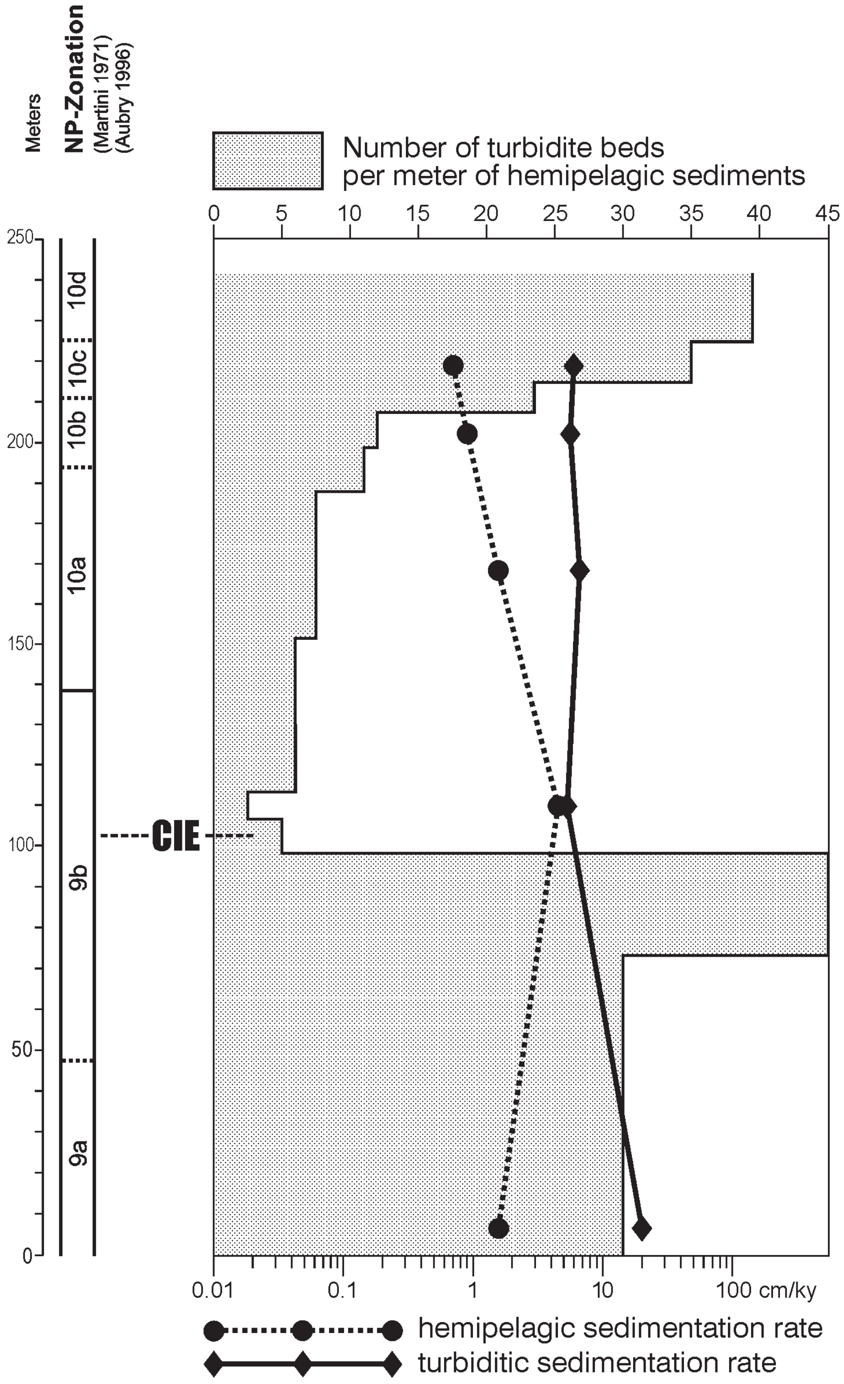

Figure 3. Relative frequency of turbidity currents and estimated turbidite and hemipelagic rates of sedimentation in nannofossil zones in the Anthering section. CIE—carbon isotope excursion,

that subzone NP10d is not complete. Therefore we did not estimate the rate of sedimentation for this subzone.

The strong increase in the rate of shale sedimentation at the CIE, by at least a factor of 3, might be partly an effect of shale deposition by bottom currents, as we found a few thin shale layers that show a transition into siltstones at their base. However, since the vast majority of shales do not display indications of redeposition, it seems unlikely that redeposition is a substantial source of the shale material. Obviously, the dramatically increased rate of hemipelagic sedimentation at the CIE suggests a high input of siliciclastic suspension into the basin. At the level of the CIE clay mineral assemblages of hemipelagic shale display a distinct increase of smectite and kaolinite at the expense of illite and chlorite (Egger et al., 2002). This indicates a decrease of bedrock erosion in the adjoining land areas. Well-developed smectitic soils with a mixture of kaolinite are mostly restricted to subtropical climates with a well-marked dry season (see Thiry, 2000, for a review). During the rainy season continental erosion of such areas is very pronounced (see van der Zwaan, 2002, for a review) and will result in a strong increase in hemipelagic sedimentation rates (Schmitz et al., 2001).

Turbiditic sedimentation rates display a decrease from 20 cm/k.y. in the lower part of zone NP9 to ~5 cm/k.y. in the upper part (Fig. 3). This is probably the result of a strong reduction of the siliciclastic sand-fraction in the turbidites: This fraction forms ~30% of the rocks in the lower part of NP9, but only 5% in the upper part of zone NP9 and in NP10. These different percentages of sandstone are used to distinguish between the older Altlengbach Formation and the younger Anthering Formation (Egger, 1995). The decrease in the input of the sand-fraction together with the coeval increase in the input of the clay-fraction suggests reduced availability of coarse material. This is consistent with the change from a temperate climate, with pronounced mechanical erosion, to a more humid climate with increased rates of soil formation.

Just before the CIE the rate of turbidite sedimentation dramatically increased and let to the deposition of the thickest turbidites of the entire Anthering Section. The calcareous nannoplankton assemblages of these thick turbidites consist almost exclusively of allochthonous Cretaceous species (Egger et al., 2000a). This suggests that during the latest Paleocene nonlithified Cretaceous sediments were mobilized as gravity flows by a very effective trigger mechanism. We suspect that the melting of gas hydrates out of the pore spaces of the Cretaceous sediments is responsible because methane can only escape from buried gas hydrate reservoirs through sediment failures (e.g., Katz et al., 1999).

Within zone NP10 no significant change in the rate of turbidite sedimentation occurred indicating that sediment accumulation in the source area of the turbidites remained stable. As the turbidites consist predominantly of penecontemporaneous calcareous plankton, it is likely that no significant change in the productivity of calcareous plankton took place within zone NP10. The concurrent increase in the relative frequency of turbiditic events was obviously a result of a decrease in the rate of hemipelagic sedimentation (Fig. 3).

Organic petrology and Rock-Eval pyrolysis

Vitrinite reflectance (~0.40% Rr) and Rock-Eval parameter Tmax (~418 °C) indicate a low maturity of the organic matter at Anthering (Table 1). As revealed by optical microscopy, the organic matter consists of marine material as well as terrestrially derived material. Samples ranging from 1.0 to 1.2 wt% TOC contain 1.8–2.5 vol% optically resolvable particles (macerals), and thus most of the organic matter is visible by optical microscopy. Marine-derived liptinite macerals, including liptodetrinite and lamalginite, are more common than sporinite, vitrinite, recycled vitrinite, and inertinite macerals of terrigenous origin. The ratio between marine and terrigenous components ranges from 1.1 to 1.5. Many liptinite macerals are characterized by orange fluorescence, which is unusal considering its low maturity, and might be an effect of oxidation. Some vitrinite particles show oxidation cracks. However, since the accompanying

TABLE 1. ROCK-EVAL AND VITRINITE REFLECTANCE DATA

Sample	TOC (wt.%)	S1 (mgHC/g rock)	S2 (mgHC/g rock)	S3 ($mgCO_2$/ g rock)	HI (mgHC/g rock)	OI ($mgCO_2$/g TOC)	T_{max} (°C)	Vitrinite Reflectance (%Rr/s)
DA66/1	0.45	0.05	0.22	0.65	48	144	–	–
EF2/98	1.22	0.19	0.82	0.27	67	23	412	0.38 / 0.05
E2/99	1.06	0.08	0.62	0.30	58	28	418	–
E1/99	1.03	0.08	0.72	0.39	69	38	418	0.36 / 0.05
JA3/99	1.01	0.08	0.58	0.46	58	46	421	0.44 / 0.06
J15/99	0.73	0.05	0.44	0.36	60	49	420	–
JF2/98	0.67	0.08	0.18	0.15	27	22	419	–
Jf3/98	0.65	0.08	0.37	0.27	57	42	418	–
J85/97	0.53	0.09	0.13	0.18	25	35	420	–
LF2/98	0.38	0.10	0.04	0.22	10	58	–	–

Note: TOC—total organic carbon; HI—hydrogen index; OI—oxygen index; Rr—mean random reflectivity; s—standard deviation.

pyrite framboids and pyritized radiolaria, which are particularly abundant in samples of outcrop E (E1/99, E2/99 and EF1/98), are unweathered oxidation must have occurred prior to the deposition of the organic debris. Reworking of vitrinite is also indicated by the common occurrence of particles with high reflectance, which does not equate with the low maturity of the samples. In particular, sample JA3/99 contains high amounts of inertinite.

Rock-Eval parameters are summarized in Table 1. HI values of the studied samples are below 70 mgHC/gTOC. In order to eliminate a possible mineral-matrix effect, S2 is plotted versus TOC (Langford and Blanc-Valleron, 1990) in Figure 4. According to the regression line, the true average hydrogen index is ~90 mgHC/gTOC. This value is typical for type III kerogen, which is essentially derived from terrestrial plants. This classification is inconsistent with the optical results, which revealed liptinite as the predominant maceral. Therefore we suspect that the low HI values are a result of the predepositional oxidation of both vitrinite and liptinite within the water column.

On the basis of the organic carbon contents of the hemipelagic shales, the Anthering section displays a threefold subdivision. Below the CIE the mean TOC value is calculated as 0.27%, from the CIE to the lower part of Zone NP10 this value increases to 0.58% while further up-section a distinct decrease to 0.16% can be identified. This varying content of organic carbon may reflect changes in primary productivity, changes in the preservation conditions of organic matter or varying oxygen levels of bottom waters.

Agglutinating foraminifera

The rich and diverse agglutinated faunas of the Anthering section offered a superb opportunity for a palecological study across the Paleocene–Eocene boundary interval in a well-dated abyssal setting. Individual samples contain up to 65 species and >700 specimens (Table 2 and Figure 5). More than 90 species were identified and grouped into four morphogroup assemblages (tubular genera, infaunal passive deposit feeders, active deposit feeders, epifaunal active herbivores and omnivores). Distributional patterns of morphogroups of agglutinating foraminifera are related, more or less directly, to food supply and food utilisation processes (Jones and Charnock, 1985).

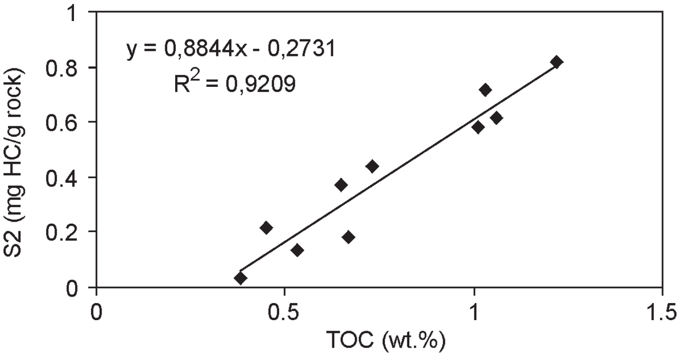

Figure 4. S2 vs. total organic carbon (TOC) diagram (Langford and Blanc-Valleron, 1990). The true average hydrogen index of samples from the Anthering Formation is 88 mgHC/gTOC.

At Anthering, tubular forms comprise the genera *Nothia, Rhabdammina, Rhizammina, Psammosiphonella* and *Bathysiphon.* These typical "flysch-type" elements have been interpreted as sessile suspension feeders (morphogroup A of Jones and Charnock). However, the ecological interpretation of some of these deep-sea genera is still under discussion (Gooday et al., 1997), e.g., the life habitat of *Nothia* has been reinterpreted as epibenthic detrivore (Geroch and Kaminski, 1992). Epi- and infaunal passive deposit feeders (morphogroup B1) comprise *Saccammina, Psammosphaera, Hormosina, Hormosinella, Trochamminoides, Paratrochamminoides, Lituotuba, Hyperammina* and *Kalamopsis.* Another epifaunal and shallow infaunal group of active deposit feeders (morphogroup B2) corresponds to the *Ammodiscus-Glomospira* assemblage of "Biofacies B" (Kuhnt et al., 1989). It consists of the genera *Ammodiscus, Glomospira* and *Rzehakina.* The B3 assemblage of epifaunal active herbivores and omnivores (*Haplophragmoides, Trochammina* s.l.) may be restricted to omnivores in this deep-sea environment. The C-morphogroup of infaunal forms (*Gerochammina, Karrerulina, Reophax, Subreophax, Spiroplectammina*) are negligible in the abyssal setting of the Anthering section. The genera *Recurvoides* and *Thalmannammina* were summarized as *Recurvoides*-assemblage. The microhabitat preferences of this assemblage are questionable. In the Cretaceous "Hatteras Fauna" of the Fardes Formation in southern Spain it cooccurs with *Glomospira* and *Ammodiscus,* and might, therefore, be indicative of oxygen deficient conditions (Kaminski et al., 1999). In our samples we did not find this correlation because the highest percentages of the *Recurvoides*-assemblage occur in high-diversity faunas without any indication of oxygen depletion. It is noteworthy that the *Recurvoides*-assemblage usually forms >10% of the agglutinated faunas within nannoplankton zone NP9, whereas in zone NP10 this percentage is much lower.

The highest diversity and the highest abundance of agglutinated specimens occur in the lower part of the section (samples NF2 to LF1). These assemblages display balanced proportions of infaunal, epifaunal and suspension feeding species. The high diversity of these agglutinated faunas is seen as typical for oligotrophic, food-limited environments where the various microhabitats are fully occupied. Several taxa have their last occurrences in this part of the section: *Ammodiscus cretaceus, Aschemocella* cf. *carpathica, A. grandis, Haplophragmoides horridus, H. suborbicularis, Hormosina trinitatensis, Karrerulina* cf. *coniformis, Paratrochamminoides heteromorphus, P. multilobus, Recurvoides walteri, Remesella varians, Rzehakina complanata, R. epigona, R. fissistomata, Spiroplectammina* cf. *dentata, Spiroplectammina spectabilis, Thalmannammina* nov. sp., *Thurammina papillata.*

Further up-section (samples J85 to JaF1) impoverished faunas with a predominance of the genus *Glomospira* appear. This

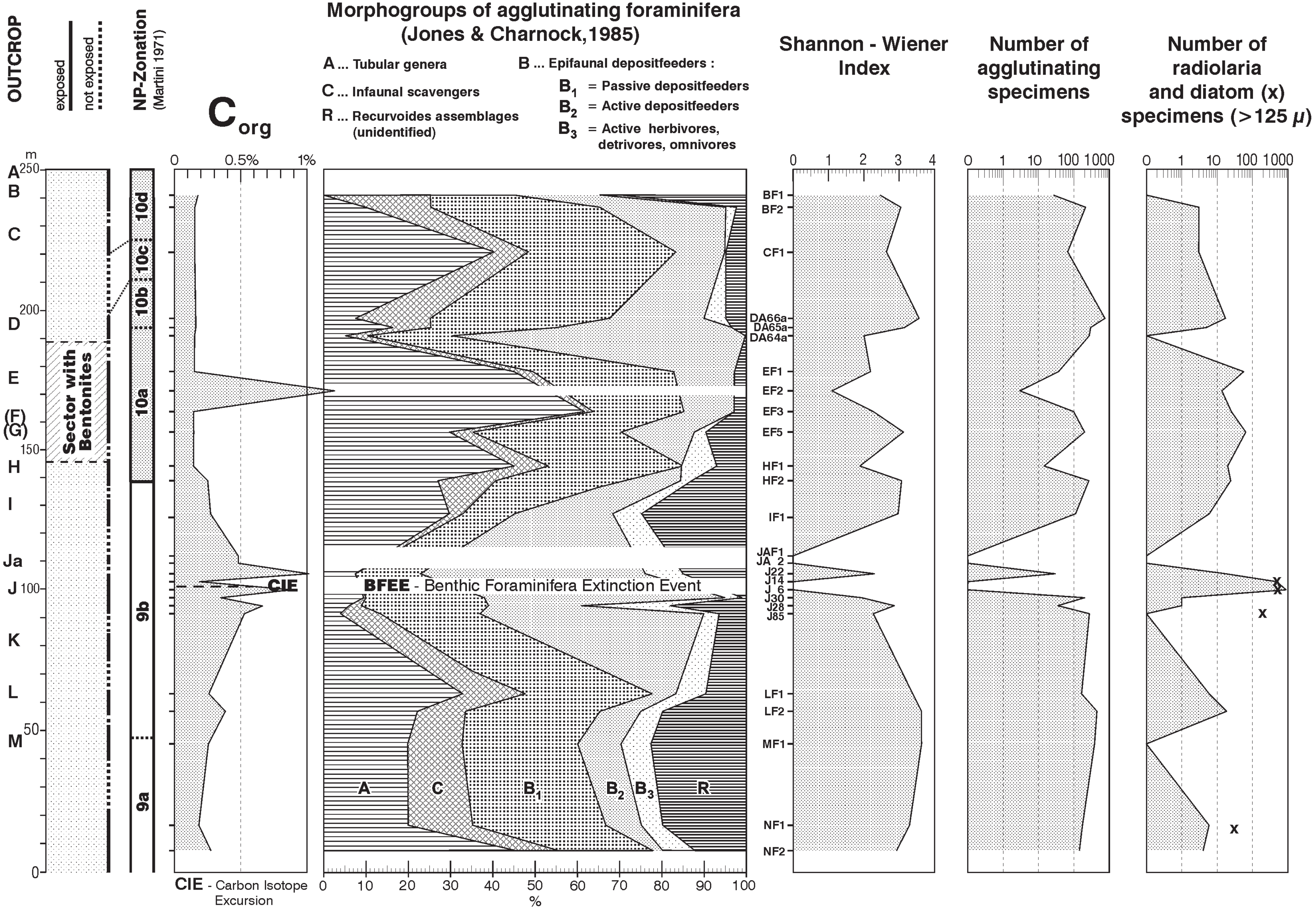

Figure 5. Distribution of organic carbon, agglutinating foraminifera and siliceous plankton within the Anthering section.

TABLE 2. DISTRIBUTION OF DEEP-WATER AGGLUTINATING FORAMINIFERA (NUMBER OF SPECIMENS) IN THE ANTHERING SECTION

sample	*Ammobaculites? sp.*	*Ammodiscus cretaceus* (REUSS)	*Ammodiscus latus* GRZYBOWSKI	*Ammodiscus planus* LOEBLICH	*Ammodiscus tenuissimus* GRZYBOWSKI	*Ammodiscus glabratus* CUSHMAN & RENZ	*Ammosphaeroidina pseudopauciloculata* (MYATLYUK)	*Annectina grzybowskii* (JURKIEWICZ)	*Aschemocella* cf. *carpathica* (NEAGU)	*Aschemocella grandis* (GRZYBOWSKI)	*Bathysiphon sp.*	*Bathysiphon? annulatus* (ANDREAE)	*Buzasina pacifica* (KRASHENINNIKOV)	*Caudammina? sp.*	*Dendrophrya sp.*	*Gerochammina conversa* (GRZYBOWSKI)	*Glomospira charoides* (JONES & PARKER)	*Glomospira diffundens* CUSHMAN & RENZ	*Glomospira glomerata* (GRZYBOWSKI)	*Glomospira gordialis* (JONES & PARKER)	*Glomospira serpens* (GRZYBOWSKI)	*Glomospira? irregularis* (GRZYBOWSKI)	*Haplophragmoides horridus* (GRZYBOWSKI)	*Haplophragmoides suborbicularis* (GRZY.)	*Haplophragmoides walteri* (GRZYBOWSKI)	*Haplophragmoides spp.*	*Hormosina* cf. *pilulifera* BRADY	*Hormosina trinitatensis* (CUSHMAN & RENZ)	*Hyperammina dilatata* GRZYBOWSKI	*Hyperammina nuda* SUBBOTINA	*Hyperammina sp.*	*Kalamopsis grzybowskii* (DYLAZANKA)	*Karrerulina* cf. *coniformis* (GRZYBOWSKI)	*Karrerulina horrida* (GRZYBOWSKI)	*Lituotuba? vermetiformis* (GRZYBOWSKI)	*Nothia communis* (PFLAUMANN)	*Nothia excelsa* (GRZYBOWSKI)	*Nothia grilli* (NOTH)	*Nothia latissima* (GRZYBOWSKI)	*Nothia robusta* (GRZYBOWSKI)	*Nothia subalpina* (PFLAUMANN)	*Paratrochamminoides deformis* (GRZYBOWSKI)	*Paratrochamminoides draco* (GRZYBOWSKI)	*Paratrochamminoides gorayskii* (GRZYBOWSKI)	*Paratrochamminoides heteromorphus* (GRZYBOWSKI)	*Paratrochamminoides multilobus* (DYLAZANKA)	*Paratrochamminoides olszewskii* (GRZYBOWSKI)	*Paratrochamminoides spp.*
BF1/98	–	–	–	–	–	–	–	1	–	–	–	–	–	–	–	4	5	–	–	1	–	–	–	–	–	–	–	–	–	–	–	–	–	–	–	–	–	–	–	–	–	–	1	–	–	–	–	–
2/98	–	–	1	20	–	–	–	–	–	–	7	–	1	–	–	7	54	3	10	6	–	5	–	–	–	–	–	–	–	13	–	–	–	8	–	–	–	–	–	–	–	–	6	–	–	–	7	9
CF1/98	–	–	–	–	–	–	–	–	–	–	–	–	–	–	–	1	6	–	1	1	–	3	–	–	–	–	2	–	–	4	–	–	–	2	–	1	–	1	–	–	18	–	1	–	–	–	–	–
DA66A	–	–	–	14	–	–	–	7	–	–	–	4	1	–	–	–	81	20	37	13	4	20	–	–	–	10	4	–	–	46	–	–	–	–	9	14	9	17	–	16	29	12	30	–	–	–	36	25
DA65A	–	–	–	3	–	–	–	15	–	–	6	2	–	–	–	–	58	17	20	4	1	6	–	–	–	–	–	–	–	13	–	1	–	–	–	–	–	4	–	10	9	2	12	–	–	–	19	9
DA64a	–	–	–	2	–	–	–	3	–	–	–	–	–	–	–	–	135	15	23	7	–	13	–	–	–	–	–	–	–	–	–	–	–	–	2	–	–	–	–	–	–	5	–	–	–	5	8	
EF1/98	–	–	–	–	–	–	–	–	–	–	–	–	–	–	–	–	5	–	–	–	–	–	–	–	–	–	–	–	–	3	–	–	–	–	–	6	–	–	–	6	3	–	–	–	–	–	–	–
EF2/98	–	–	–	–	–	–	–	–	–	–	–	–	–	–	–	–	–	–	–	–	–	–	–	–	–	–	–	–	–	1	–	–	–	–	–	–	1	–	–	–	–	–	–	–	–	–	–	–
EF3/98	–	–	2	1	–	–	–	–	–	–	–	–	–	–	–	–	6	–	1	1	–	–	–	–	–	–	–	–	–	–	–	–	–	–	–	9	–	1	–	15	30	–	1	–	–	–	–	4
EF5/98	–	–	–	2	–	–	–	1	–	–	–	1	–	–	–	–	22	7	8	3	–	8	–	–	–	–	–	–	–	–	–	–	–	–	4	1	–	6	–	22	19	–	12	–	–	–	13	8
HF1/98	–	–	–	–	–	–	–	–	–	–	–	–	–	–	–	–	1	–	–	–	–	1	–	–	–	–	–	–	–	–	–	–	–	–	–	–	–	–	–	2	5	–	1	–	–	–	–	2
HF2/98	–	–	–	3	–	–	1	–	–	–	9	–	2	–	–	–	32	–	12	1	–	3	–	–	–	3	1	–	–	4	–	–	–	–	–	–	8	5	–	7	28	–	13	–	–	–	13	–
IF1/98	–	–	–	1	–	–	–	–	–	–	–	–	3	–	–	–	14	2	2	4	1	1	–	–	–	1	–	–	–	–	–	–	–	–	–	4	–	7	–	7	11	–	1	2	–	–	3	–
JaF1/98	–	–	–	–	–	–	–	–	–	–	–	–	–	–	–	–	–	–	–	–	–	–	–	–	–	–	–	–	–	–	–	–	–	–	–	–	–	–	–	–	2	–	–	–	–	–	–	–
J22/98	–	–	–	–	–	–	–	–	–	–	–	–	3	–	–	–	2	1	–	2	–	–	–	–	–	2	–	–	–	–	–	–	–	–	–	–	–	–	–	–	–	–	–	–	–	–	–	–
J17/98	–	–	–	–	–	–	1	–	–	–	–	–	–	–	–	–	3	–	–	3	–	2	–	–	–	1	–	–	–	–	–	–	–	–	–	–	–	–	–	–	1	–	–	–	–	–	–	–
J9/97	–	–	–	–	–	–	–	–	–	–	–	–	–	–	–	–	1	1	–	1	–	–	–	–	–	–	–	–	–	–	–	–	–	–	–	–	–	–	–	–	–	–	–	–	–	–	–	–
J30/97	–	–	–	2	–	–	2	–	–	–	–	–	2	–	–	–	85	6	–	22	–	1	–	–	–	7	–	–	–	12	2	–	–	–	–	–	2	–	–	–	–	–	–	–	–	–	–	–
J28/98	–	–	–	–	–	–	–	–	–	–	–	–	–	–	–	–	3	–	–	2	2	1	–	–	2	2	2	–	–	–	–	–	–	–	–	–	–	–	–	–	–	–	–	–	–	–	–	–
J85/97	–	–	–	2	2	–	4	–	–	–	1	–	6	–	–	–	68	37	–	18	–	1	–	–	–	3	–	–	–	7	–	–	1	1	–	–	–	4	–	–	–	–	–	–	–	–	–	–
LF1/98	–	–	–	1	–	–	1	–	9	8	6	–	5	–	–	–	–	–	–	1	2	4	–	–	3	–	4	3	1	1	–	–	–	–	–	–	7	12	–	1	–	–	–	–	–	1	3	3
LF2/98	–	14	4	–	6	1	15	5	3	21	–	–	12	2	2	–	–	1	–	–	9	21	–	1	10	8	18	–	–	2	1	2	–	–	–	28	5	–	–	3	12	–	2	–	9	1	8	1
MF1/98	–	5	2	–	4	4	1	6	–	6	–	–	9	4	8	20	3	–	–	1	13	10	–	1	18	3	17	1	–	1	9	–	–	–	1	11	4	–	–	6	11	–	7	–	–	–	2	9
NF1/98	–	–	–	2	–	–	–	–	–	6	–	–	3	–	–	2	5	1	–	–	4	6	–	–	–	7	12	–	–	5	–	3	1	–	1	5	–	3	–	–	6	–	–	–	–	–	–	3
NF2/98	3	–	–	–	–	–	–	1	–	3	3	–	2	–	–	–	–	–	–	2	–	5	3	–	–	–	7	–	–	–	–	–	–	–	–	1	–	27	7	1	4	–	–	–	–	–	–	4

TABLE 2. *Continued*

sample	*Plectorecurvoides parvus* KRASHENINNIKOV	*Psammosiphonella cylindrica* (GLAESSNER)	*Psammosiphonella* sp.	*Psammosphaera irregularis* (GRZYBOWSKI)	*Recurvoidella lamella* (GRZYBOWSKI)	*Recurvoides anormis* MYATLYUK	*Recurvoides immane* (GRZYBOWSKI)	*Recurvoides nucleolus* (GRZYBOWSKI)	*Recurvoides pseudoregularis* MYATLYUK	*Recurvoides* cf. *recurvoidiformis* NEAGU & TOCOR.	*Recurvoides retroseptus* (GRZYBOWSKI)	*Recuvoides smugarensis* MYATLYUK	*Recurvoides varius* MYATLYUK	*Recurvoides walteri* (GRZYBOWSKI)	*Recurvoides* spp.	*Remesella varians* (GLAESSNER)	*Reophax elongatus* (GRZYBOWSKI)	*Reophax nodulosus* (GRZYBOWSKI)	*Rhabdammina* spp.	*Rhizammina* cf. *algaeformis* BRADY	*Rhizammina* spp.	*Rzehakina complanata* (GRZYBOWSKI)	*Rzehakina epigona* (RZEHAK)	*Rzehakina fissistomata* (GRZYBOWSKI)	*Saccammina grzybowskii* (SCHUBERT)	*Saccammina placenta* (GRZYBOWSKI)	*Silicobathysiphon* spp.	*Spiroplectammina* cf. *dentata* (ALTH)	*Spiroplectammina spectabilis* (GRZYBOWSKI)	*Subreophax pseudoscalaria* SAMUEL	*Subreophax scalaria* (GRZYBOWSKI)	*Subreophax splendidus* (GRZYBOWSKI)	*Subreophax* spp.	*Thalmannammina subturbinata* (GRZYBOWSKI)	*Thalmannammina* n.sp. (large)	*Thurammina papillata* BRADY	*Trochammina?* spp.	*Trochamminoides dubius* (GRZYBOWSKI)	*Trochamminoides folius* (GRZYBOWSKI)	*Trochamminoides grzybowskii* KAMINSKI & GEROCH	*Trochamminoides proteus* (KARRER)	*Trochamminoides septatus* (GRZYBOWSKI)	*Trochamminoides subcoronatus* (GRZYBOWSKI)	*Trochamminoides variolarius* (GRZYBOWSKI)	*Trochamminoides* spp.
BF1/98	–	–	–	–	4	–	–	3	–	–	–	–	–	–	4	–	2	–	–	–	–	–	–	–	1	–	–	–	–	–	1	–	–	–	–	–	–	2	1	–	–	–	–	–	2
BF2/98	–	4	–	–	–	–	–	–	1	–	–	–	–	–	1	–	–	–	–	17	4	–	–	–	2	3	1	–	–	–	23	3	8	5	–	–	1	12	14	–	6	–	15	–	2
CF1/98	–	–	–	–	–	–	–	–	–	–	–	–	–	–	2	–	–	–	–	–	6	–	–	–	2	4	–	–	–	–	1	–	1	1	–	–	–	2	–	–	–	–	2	2	–
DA66A	–	–	–	4	19	–	–	–	–	–	1	9	–	–	9	–	11	29	6	13	5	–	–	–	15	23	14	–	–	7	30	20	33	18	–	–	2	15	34	–	1	–	28	9	2
DA65A	–	4	–	–	1	–	–	–	–	–	–	1	–	–	4	–	4	6	–	4	5	–	–	–	–	4	1	–	–	–	5	13	–	4	–	–	–	5	12	–	–	–	4	13	–
DA64a	–	1	–	–	–	–	–	–	–	–	–	–	–	–	–	–	–	–	1	–	6	–	–	–	–	1	7	–	–	2	–	–	6	–	–	–	–	13	–	–	–	–	13	–	–
EF1/98	–	–	–	5	–	–	–	–	–	–	–	–	–	–	–	–	–	–	–	–	–	–	–	–	–	1	–	–	–	–	–	1	–	1	–	–	–	1	–	–	–	–	–	2	–
EF2/98	–	–	–	–	–	–	–	–	–	–	–	–	–	–	1	–	–	–	–	–	–	–	–	–	–	–	–	–	–	–	–	–	–	–	–	–	–	–	–	–	–	–	–	–	–
EF3/98	–	–	–	7	–	–	–	–	–	–	–	2	–	–	–	–	–	–	–	7	–	–	–	–	–	7	–	–	–	–	–	–	–	1	–	–	–	2	–	–	–	–	–	–	–
EF5/98	–	–	3	4	–	–	3	–	–	–	2	4	–	–	4	–	–	–	–	4	–	–	–	–	3	5	–	–	–	–	4	4	1	7	–	–	–	2	–	–	1	–	–	8	–
HF1/98	–	–	–	–	–	–	–	–	–	–	–	–	–	–	1	–	–	–	2	–	–	–	–	–	–	–	–	–	–	–	–	–	–	–	–	–	–	–	–	–	–	–	–	–	–
HF2/98	8	–	8	–	–	–	7	–	–	–	–	5	–	–	5	–	–	–	–	–	2	–	–	–	9	8	–	–	–	4	–	26	1	4	–	–	–	–	11	–	1	–	1	–	–
IF1/98	10	–	–	1	1	–	–	6	–	–	–	4	–	–	10	–	–	–	–	–	3	–	–	–	4	–	–	–	–	–	–	1	1	3	–	–	–	1	–	–	–	–	–	–	–
JaF1/98	–	–	–	–	–	–	–	–	–	–	–	–	–	–	–	–	–	–	–	–	–	–	–	–	–	–	–	–	–	–	–	–	–	–	–	–	–	–	–	–	–	–	–	–	–
J22/98	–	–	–	–	1	–	–	–	–	–	–	–	–	–	2	–	–	–	–	–	4	–	–	–	5	2	–	–	–	–	–	–	–	–	–	–	3	–	–	–	–	–	–	–	–
J17/98	–	–	–	–	–	–	–	–	–	–	–	–	–	–	2	–	–	–	–	–	–	–	–	–	2	–	–	–	–	–	–	–	–	–	–	–	–	–	–	–	–	–	–	–	–
J9/97	–	–	–	–	–	–	–	–	–	–	–	–	–	–	2	–	–	–	–	–	–	–	–	–	2	–	–	–	–	–	–	–	–	–	–	–	–	–	–	–	–	–	–	–	–
J30/97	–	–	6	–	–	–	–	–	–	–	–	–	–	–	2	–	–	–	–	11	–	–	–	–	41	1	–	–	–	–	–	1	–	–	–	–	1	–	–	–	–	–	–	–	–
J28/98	–	–	2	1	–	–	1	–	–	–	1	–	–	–	1	–	–	–	–	–	–	–	–	–	1	1	–	–	–	–	–	–	1	1	–	–	–	1	–	–	2	–	–	1	–
J85/97	–	–	–	–	1	–	–	–	–	–	–	–	–	–	11	–	–	–	3	–	–	–	–	–	49	1	2	–	–	–	15	6	–	–	–	–	1	–	–	–	–	–	–	–	–
LF1/98	–	5	6	11	–	–	–	–	1	–	–	–	–	–	5	–	1	–	14	–	–	–	1	–	5	6	–	–	–	–	1	1	3	3	6	–	3	2	2	–	1	–	–	1	–
LF2/98	–	6	23	13	–	7	7	–	–	5	–	–	1	–	21	–	–	–	14	–	–	1	1	–	7	24	2	–	1	2	10	6	6	–	25	1	1	4	7	–	4	–	4	–	–
MF1/98	–	–	10	–	–	3	7	–	–	–	–	–	2	1	9	–	–	2	18	–	17	–	1	1	4	23	3	–	–	–	8	3	10	–	37	–	6	2	5	–	1	–	13	1	1
NF1/98	–	2	4	–	–	–	–	–	–	–	3	5	1	3	20	–	–	1	13	–	2	–	–	–	6	13	–	1	11	–	1	1	1	–	4	–	–	–	3	–	–	1	–	–	–
NF2/98	–	–	5	–	–	–	–	–	3	–	5	–	–	–	11	1	–	–	17	–	–	–	–	–	–	6	–	–	2	–	–	1	2	–	–	1	–	–	1	–	–	–	2	2	1

"*Glomospira* event" has been observed at numerous localities in the Tethys and northern North Atlantic (see Kaminski et al., 1996, for a review). Kaminski et al. (1989) speculated that the predominance of *Glomospira* indicates areas of high surface productivity that caused low oxygen levels at the seafloor. However, this assemblage occurs also in well-oxidized sediments and, therefore, it may be opportunistic rather than a reliable indicator for high productivity (Galeotti et al., 2000; Kaminski et al., 1996). With the onset of the CIE, even this opportunistic assemblage disappeared and over a period of at least 180 000 yr the benthic communities suffered severely from unfavorable habitat conditions.

Between samples HF2 to EF1 the majority of the hemipelagic layers have an organic carbon content between 0.14% and 0.17% (0.15% on average), but several black shale layers (up to 1.22% TOC) occur. This suggests periodic eutrophication of the sea water probably by volcanic ashfall as closely spaced bentonites were found in that part of the section (Egger et al., 2000a). The black shales are usually devoid of benthic foraminifera and contain common framboidal pyrite indicating anoxic conditions (Egger et al., 1997). The agglutinating faunas of these layers are not as rich and diverse as those from further down the section. *Glomospira glomerata* has its first appearance in this part of the section. The faunal assemblage changed to a predominance of passive deposit feeders (B1-assemblage) and tubular genera (A-assemblage). These assemblages are dominant along the continental rises where bottom currents or distal turbidity currents occur (Kaminski et al., 1996).

In the uppermost part of the Anthering section (samples DA64a to BF1) a strong increase in the number of species and specimens of the DWAF, with relatively balanced assemblages, occurs indicating the return of ecological conditions similar as those at the base of the section.

Siliceous plankton

Throughout the Anthering section the fossil remains of siliceous plankton (radiolaria, diatoms as well as rare ebridians and silicoflagellates) have been replaced by pyrite. Silica dissolution prior to this replacement, and damage caused by the pressure of pyrite crystals growing inside the shells, can make identification difficult. In particular, radiolarians are very poorly preserved and are all taxonomically indeterminate spheroidal or lenticular spumellarians (Christopher Hollis, 2001, personal commun.). If pyrite fillings only are preserved, the outline and shape of diatom frustules can be recognized, but a specific and often generic determination is impossible. However, in the more robust frustules, even relatively fine pores and cribra covering the areolae are preserved, and thus allow species determination.

Most samples have diatom floras dominated by the taxa *Paralia sulcata* var. *biseriata, Paralia sulcata* var. *crenulata, Coscinodiscus antiquus,* and by species of the genera *Auloplicata* and *Stephanopyxis.* The recent relatives of the latter two genera occur in coastal-neritic as well as in oceanic environments. This may also be the case for the less common species of the genera *Hemiaulus* (e.g., *H. peripterus), Actinoptychus* and *Sceptroneis.* Species of the genus *Trochosira,* which are also rather rare, are considered to have been fully planktonic, whereas specimens of *Craspedodiscus, Trinacria, Sheshukovia* and *Aulacodiscus* probably indicate a coastal-neritic environment. Other genera can be considered to have been fully benthic, e.g., species of the genera *Auliscus* and *Arachnodiscus.* In neritic assemblages, resting spores should be abundant, but in the studied samples only single specimens of resting spores were found. These belong to the form groups *Xanthiopyxis, Pterotheca* and *Bicornis.* As resting spores are most resistant to dissolution, their scarcity indicates that the encountered diatoms represent an oceanic assemblage (Fenner, 1994). The minor admixture of coastal and neritic specimens may have been caused by storm events that whirled up freshly deposited sediment in shallow regions, which thereafter settled out from suspension beyond the shelf edge.

Dinoflagellates

Information on the distribution of organic-walled dinoflagellate cysts in the Anthering section has previously been briefly published by Egger et al. (1997, 2000a), Heilmann-Clausen and Egger (2000) and Crouch et al. (2001). With results obtained during the present study the data can be summarized as follows. Common genera ans species occurring throughout the section are *Apectodinium* spp., *Areoligera* spp., *Glaphyrocysta* spp., *Spiniferites* spp., *Polyspaeridium zoharyi, Homotryblium tenuispinosum, Operculodinium centrocarpum,* and *Phthanoperidinium crenulatum. Lingulodinium machaerophorum* occurs sporadically and is usually rare.

The overall composition of the dinoflagellate assemblages allows a simple subdivision of the section into three parts: The lower and upper interval are characterized by generally low dominance and relatively high species richness. These two intervals are separated by a middle interval coinciding with the CIE (outcrops J and JA). There the genus *Apectodinium,* which usually accounts for 5%–20% of the dinoflagellate assemblages, is dominant and reaches abundances up to 69% in hemipelagic samples. The genus *Apectodinium* includes several intergrading species, which form a closely related group (Harland, 1979). In spite of the strong dominance, the species richness remains relatively high within the CIE interval.

Quantitative dinoflagellate cyst data from hemipelagic layers at outcrop J (Fig. 6) reveal there is a 10-fold to 40-fold increase in the total number of cysts within the CIE interval (where *Apectodinium* dominates). Above the CIE, counts reveal fluctuations in cyst numbers with a general trend toward reduction, which parallel the declining percentages of *Apectodinium.* The total number of cysts is low in sample J4 from the CIE-interval, with dominant *Apectodinium,* but this sample is from a layer with a minimum in the TOC (Fig. 6) which suggests increased oxygenation at this level. The *Apectodinium* percentages are in-

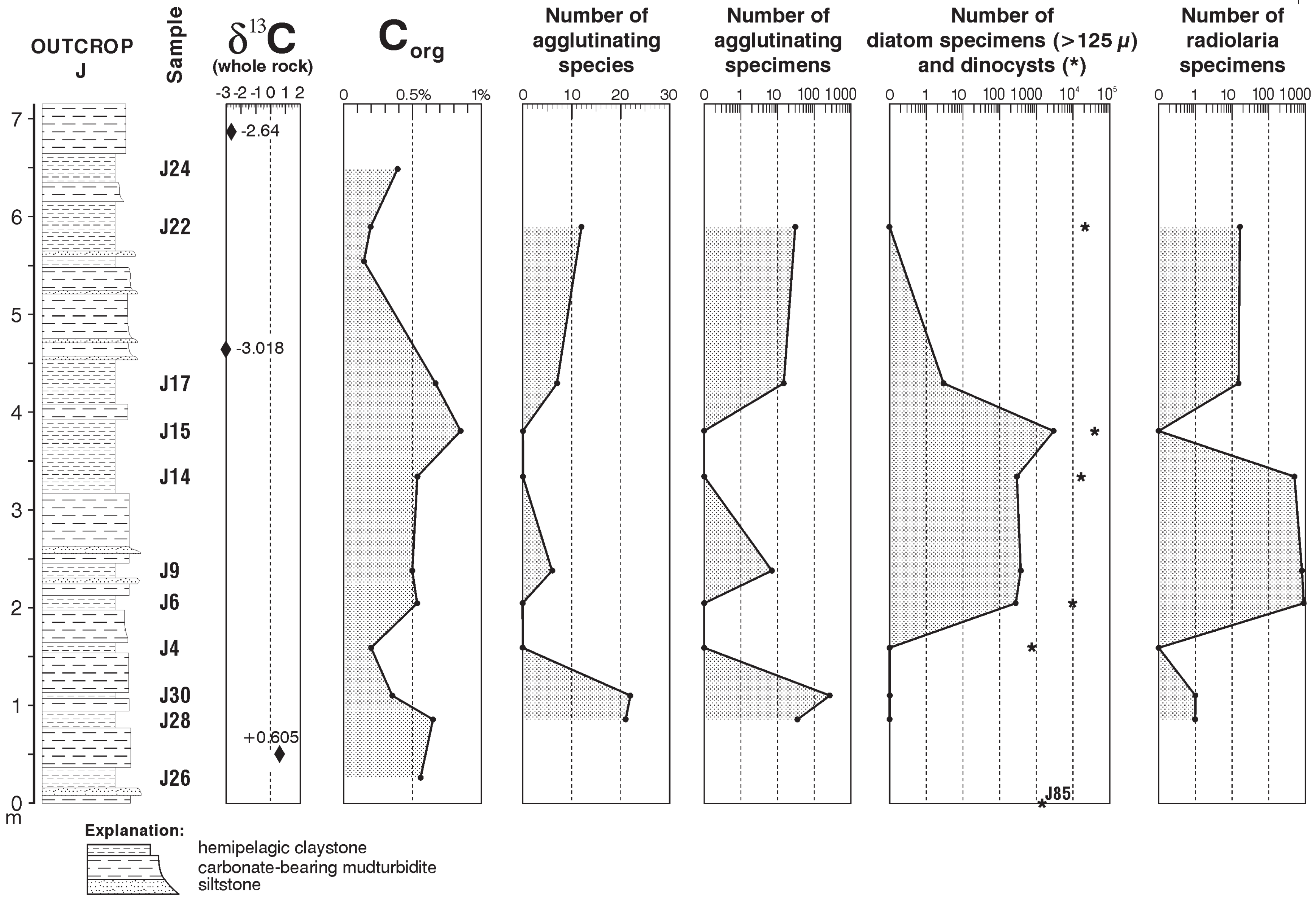

Figure 6. Detailed section of the onset of the negative carbon isotope event (CIE) displaying abundances of agglutinating foraminifera and siliceous plankton in 200 g sediment and abundances of dinoflagellates in 1 g sediment. Sample J85 was taken ~4 m below the base of the measured section.

creased in sample J26 (33%) and J28 (62%), but no data of absolute dinoflagellate abundances are available for these two samples.

Relying on information from modern cyst production (e.g., Dale, 1996), the Anthering Section must have been deposited below neritic waters, or waters that originated in the neritic zone. The genus *Impagidinium,* which is today purely oceanic, is present in several samples (especially in outcrop N), but usually rarer than 1%–2%. Such low occurrences indicate the neritic/oceanic boundary interval (Dale, 1996). It should be noted that the boundary between neritic and oceanic waters today does not strictly follow bathymetry and presence of neritic waters need not conflict with the interpretation of the depositional environment at Anthering being an abyssal basin floor (Egger et al., 2000a). It is also well known that neritic cysts are today transported over long distances with currents, and are deposited in various basinal parts of the Atlantic Ocean (e.g., Dale, 1996).

The continuous presence of *Polysphaeridium zoharyi* and *Homotryblium tenuispinosum* is evidence of a rather constant, and significant, mixing of the water masses at Anthering. *Polysphaeridium zoharyi* today mainly characterizes equatorial lagoons (Dale, 1996), and the extinct *Homotryblium* is a dominant form in several well-documented inner neritic, probably lagoonal settings of various ages (e.g., Köthe, 1990; Brinkhuis, 1994; Dybkjær and Rasmussen, 2000; and personal observation of Heilmann-Clausen in the basal Oligocene Heide Sand, Belgium).

DISCUSSION

The main factors controlling the abundance of dinoflagellate cysts and other organic matter in sediments are oxygenation of bottom waters, primary productivity, and rate of sedimentation. The latter two factors are also essential for the preservation of siliceous plankton, which is strongly influenced by dissolution, because ocean waters are highly undersaturated with respect to silica. At Anthering, our calculations of sedimentation rate provide evidence for a pronounced increase in the rate of hemipelagic sedimentation with the onset of the CIE and the coeval benthic foraminifera extinction event indicates dysoxic to anoxic conditions at the seafloor. The increase in the number of dinoflagellate cysts and siliceous plankton, and the increase in the total amount of organic carbon in the hemipelagic sediment at the level of the CIE, might be a result of these factors, at least in part. However, an increase in the rate of sedimentation, and a decrease in the oxygenation of bottom waters, cannot explain the changes in the composition of microfossil assemblages within the CIE-interval.

In 4 out of 32 samples abundant specimens of pyritized large diatoms (>125 µm) of the genera *Craspedodiscus* and *Trinacria* were found. They are restricted to samples J9, J14, J15 and J17 immediately above the CIE. These samples represent 1.30 m of shale, equivalent to an episode of 30 k.y. according to our estimated sedimentation rate. In this part of the section, the preservation of siliceous plankton is much better than in other parts at similar sedimentation rates. However, the occurrence of large diatoms cannot just be a matter of preservation because due to their size, these specimens should be less prone to dissolution than small diatoms (Mitlehner, 1996). Therefore, we assume that high abundance of siliceous plankton caused the better preservation as the result of an increased input of biosiliceous particles. This is consistent with the large quantity of small, roundish diatoms (not identifyable with the light microscope) and common specimens of the genus *Hemiaulus,* which suggest high surface water productivity (Fenner, 1991).

The occurrence of *Craspedodiscus* spp. and *Trinacria* spp. in deep-water deposits at Anthering is highly remarkable as these genera are usually restricted to neritic environments. We can rule out redeposition of these specimens because in that case, resting spores and benthic species would have been redeposited in considerable amounts. Their scarcity indicates an oceanic assemblage (Fenner, 1994). This suggests that water-depth was not the limiting factor for the occurrence of *Craspedodiscus* spp. and *Trinacria* spp. Probably, the preference of these genera for neritic settings was due to the higher level of dissolved nutrients in these areas.

The high abundance of large diatom specimens correlates with the onset of the *Apectodinium* acme. This *Apectodinium* event may reflect exceptionally high sea-surface temperatures and/or a significant increase in surface-water productivity (Brinkhuis et al., 1994; Bujak and Brinkhuis, 1998; Crouch et al., 2001). Data from the southern, marginal part of the North Sea Basin suggest that the distribution of *Apectodinium* was also strongly influenced by distance from the coast. This is evident from a comparison of abundances in post-CIE deposits within the NP10 chronozone in three boreholes in the Hamburg region: *Apectodinium* is more abundant in the relatively coastal Gartow and Lingen-1 boreholes (Köthe, 1990) but much rarer in the more offshore Wursterheide borehole (Heilmann-Clausen and Costa, 1989). It thus appears that *Apectodinium* flourished in certain inner neritic environments, as formerly suggested by Stover et al. (1996). However, during the CIE extreme abundances of *Apectodinium* were found also in the central parts of the North Sea basin. There, organic-rich, anoxic layers in part of the Sele Formation, and equivalent Stolleklint Clay (Heilmann-Clausen and Schmitz, 2000), indicate that waters in the entire basin were nutrient-rich with a high plankton productivity.

It can be summarized that the concurrent acmes of predominantly neritic organisms (*Craspedodiscus* spp., *Trinacria* spp. and *Apectodinium* spp.) in the sedimentary record of the open marine setting at Anthering are most likely an effect of a strong increase in nutrient supply. Biogene carbonate production primarily controls the volume of sediment available for incorporation in turbidity currents. At Anthering, the rate of turbidite sedimentation remained stable during zone NP10, suggesting that the productivity of calcareous plankton did not change, apparently in disagreement with the assumed high productivity of dinoflagellates and siliceous plankton. This is, however, consistent with modern oceans (Ziveri et al., 1995), where in the presence of high nutrient levels, diatoms and dinoflagellates are the most abundant phytoplankton and the productivity and flux of coccolithophorides decreases.

The benthic foraminifera extinction event (BFEE) in the upper part of Zone NP9 and its potential causes, have been discussed extensively (see Thomas, 1998, for a review). Around the CIE at Anthering, the morphogroup B assemblage (*Glomospira*-fauna) dominates. The ecological significance of this assemblage is still unclear. *Glomospira* may be an opportunistic genus in the sense that it is a good recolonizer of azoic sediments (Kaminski et al., 1996).

CONCLUSIONS

The Anthering Section provides good evidence for an increase in the rate of hemipelagic sedimentation and primary surface productivity at the level of the CIE. This suggests that eutrophication of surface waters was triggered by enhanced continental runoff as a result of the establishment of subtropical climate conditions. The associated increase in the input of nutrients to the ocean basins was enough to have affected even open marine settings. This increased nutrient supply caused the migration of planktonic taxa, like *Apectodinium* spp., *Trinacria* spp. and *Craspedodiscus* spp., from neritic environments to settings further away from the coast. As a result of the associated episodically increased flux of organic carbon to the seafloor, a total extinction of deep-sea benthic foraminifera faunas took place.

ACKNOWLEDGMENTS

For their helpful reviews and comments we are grateful to Wolfgang Kuhnt, Simonetta Monechi, James Powell and Ellen Thomas. We are indebted to Christopher Hollis for examining the radiolarian faunas, Miroslav Bubik for discussion and comparative material of DWAF, and Peter Klein for the determination of total organic carbon contents. We thank Silvia Spezziferri and Johann Hohenegger for their help in the statistical interpretation of the DWAF and Jacek Ruthner for his technical assistance in preparing the figures.

REFERENCES CITED

Aubry, M.-P., 1996, Toward an upper Paleocene–lower Eocene high-resolution stratigraphy based on calcareous nannofossil stratigraphy: Israel Journal of Earth Sciences, v. 44, p. 239–253.

Aubry, M.-P., Berggren, W.A., Stott, L., and Sinha, A., 1996, The upper Paleocene–lower Eocene stratigraphic record and the Paleocene-Eocene boundary carbon isotope excursion: Implications for geochronology, *in* Knox, R.W.O'B., et al., eds., Correlation in the early Paleogene in northwest Europe: Geological Society [London] Special Publication 101, p. 353–380.

Bains, S., Norris, R.D., Corfield, R.M., and Faul, K.L., 2000, Termination of global warmth at the Paleocene–Eocene boundary through productivity feedback: Nature, v. 407, p. 171–174.

Brinkhuis, H., 1994, Late Eocene to early Oligocene dinoflagellate cysts from the Priabonian type-area (Northeast Italy): Biostratigraphy and paleoenvironmental interpretation: Palaeogeography, Palaeoclimatology, Palaeoecology, v. 107, p. 121–163.

Brinkhuis, H., Romein, A.J.T., Smit, J., and Zachariasse, J.-W., 1994, Danian–Selandian dinoflagellate cysts from lower latitudes with special reference to the El Kef section, northwest Tunisia: GFF, v. 116, p. 46–48.

Bujak, J.P., and Brinkhuis, H., 1998, Global warming and dinocyst changes across the Paleocene–Eocene epoch boundary, *in* Aubry, M.-P., et al., eds., Late Paleocene–early Eocene: New York, Columbia University Press, p. 277–295.

Butt, A., 1981, Depositional environments of the Upper Cretaceous rocks in the northern part of the Eastern Alps: Cushman Foundation for Foraminiferal Research, Special Publication, v. 20, 121 p.

Bybell, L.M., and Self-Trail, J.M., 1994, Evolutionary, biostratigraphic, and taxonomic study of calcareous nannofossils from a continuous Paleocene–Eocene boundary section in New Jersey: U.S. Geological Survey Professional Paper 1554, 73 p.

Crouch, E.M., Heilmann-Clausen, C., Brinkhuis, H., Morgans, H.E.G., Rogers, K.M., Egger, H., and Schmitz, B., 2001, Global dinoflagellate event associated with the late Paleocene Thermal Maximum: Geology, v. 29, p. 315–318.

Dale, B., 1996, Dinoflagellate cyst ecology: Modeling and geological applications, *in* Jansonius, J., and McGregor, D.C., eds., Palynology: Principles and applications: American Association of Stratigraphic Palynologists Foundation, v. 3, p. 1249–1275.

Dickens, G.R., O'Neil, J.R., Rea, D.K., and Owen, R.M., 1995, Dissociation of oceanic methane hydrate as a cause of the carbon isotope excursion at the end of the Paleocene: Paleoceanography, v. 10, p. 965–971.

Dickens, G.R., Thomas, E., and Bralower, T.J., 2001, A low productivity model for excess barite accumulation during the late Paleocene thermal maximum, *in* Ash, A.W., and Wing, S.L., eds., Climate and biota of the early Paleogene: International Meeting July 3–8, 2001, Northwest College, Powell, Wyoming, USA, Abstract volume, p. 27.

Draxler, I., 2000, First results on pollen and spores from the Paleocene–Eocene boundary interval of the Anthering section, Austria: GFF, v. 122, p. 42.

Dybkjær, K., and Rasmussen, E.S., 2000, Palynological dating of the Oligocene–Miocene successions in the Lillebælt area, Denmark: Bulletin of the Geological Society of Denmark, v. 47, p. 87–103.

Egger, H., 1995, Die Lithostratigraphie der Altlengbach-Formation und der Anthering-Formation im Rhenodanubischen Flysch (Ostalpen, Penninikum): Neues Jahrbuch für Geologie und Paläontologie Abhandlungen, v. 196, p. 69–91.

Egger, H., Bichler, M., Draxler, I., Homayoun, M., Huber, H.-J., Kirchner, E.Ch., Klein, P., and Surenian, R., 1997, Mud turbidites, black shales, and bentonites from the Paleocene–Eocene boundary: The Anthering Formation of the Rhenodanubian flysch (Austria): Jahrbuch Geologische Bundesanstalt, v. 140, p. 29–45.

Egger, H., Heilmann-Clausen, C., and Schmitz, B., 2000a, The Paleocene–Eocene boundary interval of a Tethyan deep-sea section and its correlation with the North Sea Basin: Société Géologique de France Bulletin, v. 171, p. 207–216.

Egger, H., Homayoun, M., and Rögl, F., 2000b, Deep-sea sedimentation and paleoproductivity in the Paleogene of a Tethyan basin: GFF, v. 122, p. 44–45.

Egger, H., Homayoun, M., and Schnabel, W., 2002, Tectonic and climatic control of Paleogene sedimentation in the Rhenodanubian Flysch basin (Eastern Alps, Austria): Sedimentary Geology, v. 152, p. 247–262.

Espitalié, J., Laporte, J.L., Madec, M., Marquis, F., Leplat, P., Paulet, J., and Boutefeu, A., 1977, Méthode rapide de caractérisation des roches mères de leur potentiel pétrolier et de leur degré d'évolution: Revue Institute France Pétrologique, v. 32, p. 23–43.

Fenner, J., 1991, Taxonomy, stratigraphy, and palaeoceanographic implications of Paleocene diatoms, *in* Ciesielski, P., and Kristoffersen, Y., eds., Proceedings of the Ocean Drilling Program, Scientific Results: Texas A & M University, College Station, Texas, USA, v. 114, p. 123–154.

Fenner, J., 1994, Diatoms of the Fur Formation, their taxonomy and biostratigraphic interpretation: Results from the Harre borehole, Danmark: Aarhus Geoscience, v. 1, p. 99–163.

Galeotti, S., Angori, E., Coccioni, R., Ferrari, G., Galbrun, B., Monechi, S., Premoli-Silva, I., Speijer, R., and Turi, B., 2000, Integrated stratigraphy acros the Paleocene–Eocene boundary in the Contessa Road section, Gubbio (central Italy): Société Géologique de France Bulletin, v. 171, p. 355–366.

Gavrilov, Y.O., Shcherbinina, E.A., and Muzylöv, N.G., 2000, A Paleogene sequence in central North Caucasus: A response to paleoenvironmental changes: GFF, v. 122, p. 51–53.

Gawenda, P., Winkler, W., Schmitz, B., and Adatte, T., 1999, Climate and bioproductivity control on carbonate turbidite sedimentation (paleocene to earliest Eocene, Gulf of Biscay, Zumaia, Spain): Journal of Sedimentary Petrology, v. 69, p. 1253–1261.

Geroch, S., and Kaminski, M.A., 1992, The morphology, palecology and systematics of Nothia excelsa (Grzybowski), a deep-water agglutinted foraminifer: Annales Societas Geologorum Poloniae, v. 62, p. 255–265.

Gooday, A.J., Shires, R., and Jones, A.R., 1997, Large, deep-sea agglutinated foraminifera: Two different kinds of organization and their possible ecological significance: Journal of Foraminiferal Research, v. 27, p. 278–291.

Harland, R., 1979, The *Wetzeliella (Apectodinium) homomorpha* plexus from the Paleogene/earliest Eocene of northwest Europe: IV International Palynological Conference, Lucknow (1976–1977), v. 2, p. 59–70.

Heilmann-Clausen, C., and Costa, L.I., 1989, Dinoflagellate Zonation of the Uppermost Paleocene? to lower Miocene in the Wursterheide Research Well, northwest Germany: Geologisches Jahrbuch, Ser. A, v. 111, p. 431–521.

Heilmann-Clausen, C., and Egger, H., 2000, The Anthering outcrop (Austria): A key section for correlation between Tethys and northwestern Europe near the Paleocene–Eocene boundary: GFF, v. 122, p. 69.

Heilmann-Clausen, C., and Schmitz, B., 2000, The late Paleocene thermal maximum δ^{13}C excursion in Denmark?: GFF, v. 122, p. 70.

Hesse, R., 1975, Turbiditic and nonturbiditic mudstone of Cretaceous flysch sections of the East Alps and other basins: Sedimentology, v. 22, p. 387–416.

Jones, R.W., and Charnock, M.A., 1985, “Morphogroups” of agglutinating foraminifera: Their life positions and feeding habits and potential applicability in (paleo)ecological studies: Revue Paleobiologique, v. 4, p. 311–320.

Kaminski, M.A., Gradstein, F.M., and Berggren, W.A., 1989, Palaeogene benthic foraminifer biostratigraphy and Palaeoecology at Site 647, southern Labrador Sea, *in* Srivstava, S.P., et al., eds., Proceedings of the Ocean Drilling Program, Scientific Results: Texas A & M University, College Station, Texas, USA, v. 105, p. 705–730.

Kaminski, M.A., Kuhnt, W., and Radley, J.D., 1996, Paleocene–Eocene deep water agglutinated foraminifera from the Numidian Flysch (Rif, Northern Morocco): Their significance for the palaeoceanography of the Gibraltar gateway: Journal of Micropalaeontology, v. 15, p. 1–19.

Kaminski, M.A., Kuhnt, W., and Moullade, M., 1999, The evolution and paleobiogeography of abyssal foraminifera since the Early Cretaceous: A tale of four faunas: Neues Jahrbuch für Geologie und Paläontologie Abhandlungen, v. 212, p. 401–439.

Katz, M.E., Pak, D.K., Dickens, G.R., and Miller, K.G., 1999, The source and fate of massive carbon input during the latest Paleocene thermal maximum: Science, v. 286, p. 1531–1533.

Kennett, J.P., and Stott, L.D., 1991, Abrupt deep-sea warming, palaeoceanographic changes, and benthic extinctions at the end of the Paleocene: Nature, v. 353, p. 225–229.

Köthe, A., 1990, Paleogene Dinoflagellates from Northwest Germany: Geologisches Jahrbuch, Serie A, v. 118, p. 3–111.

Kuhnt, W., Kaminski, M.A., and Moullade, M., 1989, Late Cretaceous deep-water agglutinated foraminiferal assemblages from the North Atlantic and its marginal seas: Geologische Rundschau, v. 78, p. 1121–1140.

Langford, F.F., and Blanc-Valleron, M.-M., 1990, Interpreting Rock-Eval pyrolysis data using graphs of pyrolyzable hydrocarbons versus total organic carbon: AAPG (American Association of Petroleum Geologists) Bulletin, v. 74, p. 799–804.

Lipps, J., Berger, W.H., Buzas, M.A., Douglas, R.G., and Ross, C.A., 1979, Foraminiferal ecology and palecology: Society of Economic Paleontologists and Mineralogists, Short Course 6, Houston, Texas, 198 p.

Lu, G., and Keller, G., 1993, The Paleocene–Eocene transition in the Antarctic Indian Ocean: Inference from planktic foraminifera: Marine Micropaleontology, v. 21, p. 101–142.

Martini, E., 1971, Standard Tertiary and Quaternary calcareous nannoplankton zonation, *in* Farinacci, A., ed., Proceedings of the 2nd Planktonic Conference, Roma, Italy, 1970: Tecnoscienza, v. 2, p. 739–785.

Mitlehner, A.G., 1996, Palaeoenvironments in the North Sea Basin around the Paleocene–Eocene boundary: Evidence from diatoms and other siliceous microfossils, *in* Knox, R.W.O’B., et al., eds., Correlation of the early Paleogene in northwestern Europe: Geological Society [London] Special Publication 101, p. 255–273.

Schmitz, B., Asaro, F., Molina, E., Monechi, S., von Salis, K., and Speijer, R., 1997a, High-resolution iridium, δ^{13}C, δ^{18}O, foraminifera, and nannofossil profiles across the latest Paleocene benthic extinction event at Zumaya, Spain: Palaeogeography, Palaeoclimatology, Palaeoecology, v. 133, p. 49–68.

Schmitz, B., Charisi, S.D., Thompson, E.I., and Speijer, R.P., 1997b, Barium, SiO_2 (excess), and P_2O_5 as proxies of biological productivity in the Middle East during the Paleocene and the latest Paleocene benthic extinction event: Terra Nova, v. 9, p. 95–99.

Schmitz, B., Pujalte, V., and Nunez-Betelu, K., 2001, Climate and sea-level perturbations during the Initial Eocene Thermal Maximum: Evidence from siliciclastic units in the Basque Basin (Ermua, Zumaia and Trabakua Pass), northern Spain: Palaeogeography, Palaeoclimatology, Palaeoecology, v. 165, p. 299–320.

Scotese, C.P., and Golanka, J., 1992, Paleogeographic atlas: Paleomap progress report: Arlington, University of Texas, 34 p.

Speijer, R.P., Schmitz, B., and van der Zwaan, G.J., 1997, Benthic foraminiferal extinction and repopulation in response to latest Paleocene Tethyan anoxia: Geology, v. 25, p. 683–686.

Stockmarr, J., 1971, Tablets with spores used in absolute pollen analysis: Pollen et Spores, v. 13, p. 615–631.

Stover, L.E., Brinkhuis, H., Damassa, S.P., De Vertuil, L., Helby, R.J., Monteil, E., Partridge, A.D., Powell, A.J., Riding, J.B., Smelror, M., and Williams, G.L., 1996, Mesozoic–Tertiary dinoflagellates, acritarchs and prasinophytes, *in* Jansonius, J., and McGregor, D.C., eds., Palynology: Principles and applications: American Association of Stratigraphic Palynologists Foundation, v. 2, p. 641–750.

Thiry, M., 2000, Palaeoclimatic interpretation of clay minerals in marine deposits: An outlook from the continental origin: Earth Science Reviews, v. 49, p. 201–221.

Thomas, E., 1998, Biogeography of the late Paleocene benthic foraminifera extinction, *in* Aubry, M.-P., et al., eds., Late Paleocene–early Eocene: New York, Columbia University Press, p. 214–235.

van der Zwan, C.J., 2002, The impact of Milankovitch-scale climatic forcing on sediment supply: Sedimentary Geology, v. 147, p. 271–294.

Wing, S.L., Bown, T.M., and Obradovic, J.D., 1991, Early Eocene biotic and climatic change in interior western North America: Geology, v. 19, p. 1189–1192.

Ziveri, P., Thunell, R.C., and Rio D., 1995, Export production of coccolithophores in an upwelling region: Results from San Pedro Basin, Southern California Borderlands: Marine Micropaleontology, v. 24, p. 335–358.

MANUSCRIPT ACCEPTED BY THE SOCIETY AUGUST 13, 2002

Printed in the USA